Supporting Information

Lewis Acid-Base Interaction-Driven Phosphodiester Hydrolysis in Single-Atom Nanozymes

Yimeng Wang,[a] Zhiling Zhu,[b]* Lina Wang [a]*

[a]*College of Environment and Safety Engineering, Qingdao University of Science and Technology, 53 Zhengzhou Road, Qingdao, Shandong 266042, China*

[b]*College of Materials Science and Engineering, Qingdao University of Science and Technology, 53 Zhengzhou Road, Qingdao, Shandong 266042, China*

Corresponding author

*E-mail: zlzhu@qust.edu.cn, lnwang2006@163.com

Supplementary and instruments

1. Materials

Dicyandiamide (DCDA, $C_2H_4N_4$, ≥96.0%), Cerium acetate ($Ce(Ac)_3 \cdot nH_2O$, 99.9%), Orthoboric acid (H_3BO_3, 98%)，Sodium hydroxide (NaOH, 98%), ethylene glycol (EG, 98%), anhydrous ethanol (99.5%), horseradish peroxidase (HRP, BR grade), glutaraldehyde (25 wt% in H_2O), N-(2 hydroxyethyl)piperazine-N'-(3-propanesulfonic acid) (HEPPS, 98%), formalin (36.0 40.0%), penicillin (98%), and gentamicin (≥590 $IU \cdot mg^{-1}$) were purchased from Sinopharm Chemical Reagent Co., Ltd. (Shanghai, China). 3',3',5,5'-tetramethylbenzidine (TMB, ≥99.0%), and 4-nitrophenyl phosphate disodium salt (P-NPP, 98%) were provided by Aladdin Chemical Reagent Co., Ltd. (Shanghai, China). Phosphate buffered saline (PBS) powder, Luria-Bertani (LB) broth, and LB agar powder were purchased from Qingdao Hope Bio-Technology Co., Ltd. (Qingdao, Shandong, China). Staphylococcus aureus (*S. aureus*, ATCC 6538) and Escherichia coli (*E. coil*, ATCC 27853) bacterial strains were obtained from Beijing microbio-logical culture collection center (BJMCC, Beijing, China). All chemicals and reagents were purchased from analytical grade and used without further purification. The ultrapure water used in all experiments met the following specifications: a resistivity of at least 18 $M\Omega\ cm^{-1}$, an electrical conductivity of no more than 0.1 $\mu s \cdot cm^{-1}$ and a total organic carbon (TOC) level of less than 10 ppb.

2. Characterization

The structures of the samples were characterized by high-resolution transmission electron microscopy (HRTEM, JEOL JEM-2010, Japan). The elemental distributions were investigated by the energy-dispersive X-ray spectrometry (EDS) mapping. Scanning electron microscope (SEM) was performed on an S-4800 instrument (Hitachi, Japan). High-resolution transmission electron microscopy (HRTEM) images of the typical samples were obtained on a Tecnai G2 F30 (Netherlands) apparatus at an accelerating voltage of 200 kV. Xray diffraction (XRD) patterns of the samples were recorded on a Bruker D8 Advance diffractometer (AXS-Bruker, German) with Cu α radiation and nickel filter (λ = 0.15406 nm), the operating voltage and current was 40 kV and 40 mA, respectively. X-ray photoelectron spectroscopy (XPS) analysis was performed on a Thermo ESCALAB 250XI multifunctional imaging electron

spectrometer (USA), using monochromatic Al K radiation (1486.6 eV) operating at an accelerating power of 15 kW. The binding energy was calibrated using a C 1s peak at 284.8 eV as standard and quoted with an accuracy of ± 0.1 eV.

3. Synthesis of Ce-NC and Ce-BNC nanozymes

Synthesis of Ce-BNC. Briefly, required amount of Boric acid (H_3BO_3) and 20 g of DCDA precursor was added into 200 mL of EG under stirring at 80 °C for 30 min to form a true solution. Then, 15 mg $Ce(CH_3COO)_3 \cdot H_2O$ as a Ce source was dissolved in 5 mL DCDA/EG solution under ultrasonic for 15 min to form a blue Ce-DCDA/EG mixture. Subsequently, the white Ce-DCDA/EG mixture was kept at temperature of 60 °C for 3 h in oven and Ce-DCDA/EG complex was obtained. This dried mixture was transferred to a ceramic crucible with cover lid and calcined in air at 650 °C for 4h with a ramp rate of 3 °C/min. After calcination, a yellowish orange compound of Ce-BNC was obtained, which was grounded into fine powder. Ce-NC powder was also prepared by using the same procedure without the addition of Boric acid.

4. Measurement of enzyme-mimicking activities of Ce-BNC

The OPH-like activity of Ce-BNC was determined at 60 °C using P-NPP as a substrate. The concentration dependence of OPH-like activity was obtained by adding different Ce-BNC concentrations (0, 10, 20, 40, 80 and 100 μg mL^{-1}) and P-NPP (1 mM) in HEPES buffer (pH 9). The absorbance at 405 nm was measured using a UV Vis spectrophotometer (U2900, Hitachi High-Technologies, Japan).

5. Steady-state kinetic analysis

The steady-state kinetic analysis of the OPH-like activity was performed at 60 °C in 1 mL of HEPES buffer (pH 9) by varying the concentration of P-NPP (0-1.0 mM) in the presence of Ce-BNC at a fixed concentration of 100 μg mL^{-1}. All the reactions were monitored by measuring changes in absorbance by a kinetic mode at 405 nm for 60 min.

The steady-state reaction rates at various concentration were derived from the change of the slopes of initial absorbance.

The data were fitted to Michaelis-Menten and Lineweaver-Burk plots using the equation:

$$v = \frac{V_{max}[S]}{K_m + [S]} \#(S1)$$

$$U_{(Nanozyme)} = \left(\frac{V}{\varepsilon \times l} \times \left(\frac{\Delta A}{\Delta t}\right)\right) \#(S2)$$

v is the total volume of the system, $\frac{\Delta A}{\Delta t}$ is the initial slope of the absorbance change, ε is the molar extinction coefficient of the oxidized P-NP product, l is the optical path length.

The kinetic parameters, K_m and v_{max} could be calculated from the double reciprocal equation. The catalytic efficiency K_{cat} was obtained from the equation(6):

$$K_{cat} = \frac{v_{max}}{[E]} \#(S3)$$

$[E]$ is the particle concentration of catalysts.

6. Specific activity

Various concentrations of Ce-BNC and Ce-NC were incubated with 140 μL of HEPES buffer (pH 9) and PNPP solutions at different concentrations (0.1, 0.2, 0.4, 0.6, 0.8, 1, and 2 mg mL^{-1}), respectively. The absorbance time curves of the above assays were recorded at 400 nm in time scan mode using a UV-Vis spectrometer (Cary 5000, Agilent Technologies Inc, USA) The specific activity (U mg^{-1}) was obtained via the following formula:

$$SA = \frac{V/(\varepsilon \times l) \times (\Delta A/\Delta t)}{m} \quad \text{(S4)}$$

V is the total volume of the reaction solution (μL); *ε* is the molar extinction coefficient of p-nitrophenol (p-NP) at 405 nm (18,000 M^{-1} cm^{-1}); *l* is the optical path length of the cuvette (cm); *A* is the absorbance after subtraction of the blank; Δ*A*/Δ*t* represents the initial rate of change in absorbance at 405 nm (min^{-1}); and *m* is the mass of SAzyme used in each assay (mg).

7. Density functional theory (DFT) calculations

All the first-principles calculations were performed by the Vienna ab initio simulation package (VASP) using the framework of DFT. The projector augmented wave (PAW) method was used to treat the effective interaction of the core electrons

and nucleus with the valence electrons and the generalized gradient approximation (GGA) in the form of Perdew-Burke-Ernzerhof (PBE) was adopted for the exchange-correlation functional. The Kohn-Sham electron wave functions were expanded using the plane-wave functions with an energy cutoff of 500 eV. The optimization was considered convergence when the spring force between adjacent images was less than 0.02 eV $Å^{-1}$, the total energy change upon two steps for the electronic self-consistent field iteration was less than $1E^{-5}$ eV, which has been confirmed to be precise enough under the convergence condition tests.

Charge transfers were calculated and analyzed using the Bader charge method. As for the adsorption case of small molecules (H_2O and O_2), the adsorption energy (E_{ad}) was defined as

$$E_{ads} = E_{absorbate/support} - (E_{absorbate} + E_{support}) \quad \text{(S5)}$$

and for the co-adsorption case, similar to the single molecular adsorption, the binding energy is defined as

$$E_{ads} = E_{absorbate/support} - (E_{absorbate1} + E_{absorbate2} + E_{support}) \quad \text{(S6)}$$

where $E_{absorbate}$, $E_{support}$, and $E_{absorbate/support}$ are the total energies of the free adsorbate, the corresponding support, and the support with the adsorbate in the same slab, respectively. All three types of energies were derived from the scf calculations using the same calculated setting parameters. With this definition, a negative value indicates an exothermic adsorption and the more negative this value is, the large interaction between molecules and the substrate has been proved. The spin value of the triplet state of oxygen was set to 1. The infrared intensity of the radical intermediates was calculated using linear response within the Density Functional Perturbation Theory (DFPT). The obtained Born files were then analyzed using the Phonopy-Spectroscopy software to derive the infrared intensity of the oxygen-containing intermediates.

8. Determination of biofilm biomass by crystal violet assay

Bacterial biofilm was determined by 48-well plate assay. 1 mL of LB culture solution was added to each well of a 48-well polystyrene culture plate and inoculated with 10 μL of overnight cultured *S. aureus* or *E. coil*. Subsequently, 20 μL of Ce-BNC at different concentrations were added to each well to achieve a final concentration of 0, 10, 20, 40 and 80 μg mL^{-1}. Buffer solution was added to the

control group. After culture at 37 ℃ for 24 h, the culture solution was sucked out, and each well of the culture plate was cleaned with sterilized ultrapure water for 3 times. The bacterial biofilms were fixed with 95% formalin for 15 min and stained with 0.1% crystal violet solution. After 20 min incubation, the wells were washed with PBS for three times to remove redundant dyes, followed by air drying for 1 h. Finally, the crystal violet-stained biofilms were assessed upon the addition of 33% acetic acid and OD590 measurement.

9. Plate counting assay

S-7 Ce-BNC (0-200 μg mL^{-1}) was mixed with fresh bacterial suspensions (1×10^7 CFU mL^{-1}) in PBS (1 mL, pH 7.4). S. *aureus* and E. *coli* suspension (1, 10^{-2}, 10^{-4}, and 10^{-6}) was then diluted and 100 μL of the solution was applied uniformly on LB agar and incubated for 24 h at 37 °C to count colonies.

10. Morphology analysis of biofilms by SEM

The morphology of biofilms after different treatments were observed by SEM. The pre-treated biofilms were washed 3 times with sterilized PBS. Subsequently, 500 μL of paraformaldehyde (4 wt%) was added to each group. After that, the biofilms were fixed at 4 °C for 4 h. The fixed biofilms were sequentially dehydrated according to the following concentrations of ethanol: 20%, 40%, 60%, 80%, and 100%. Each sample was prepared by sputter coating and visualized by SEM at the acceleration voltage of 10 kV

Supplementary Figures

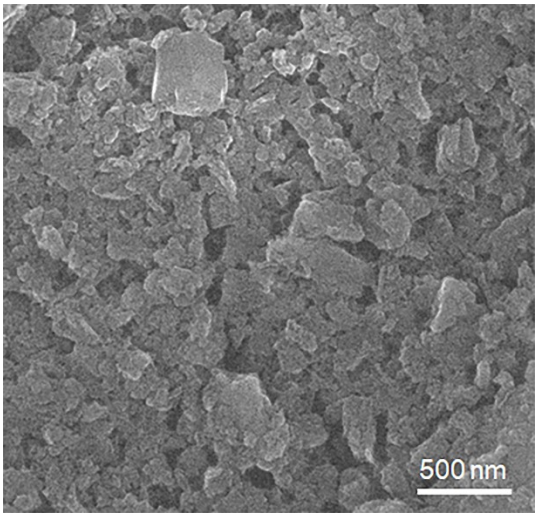

Figure S1. SEM image of Ce-BNC.

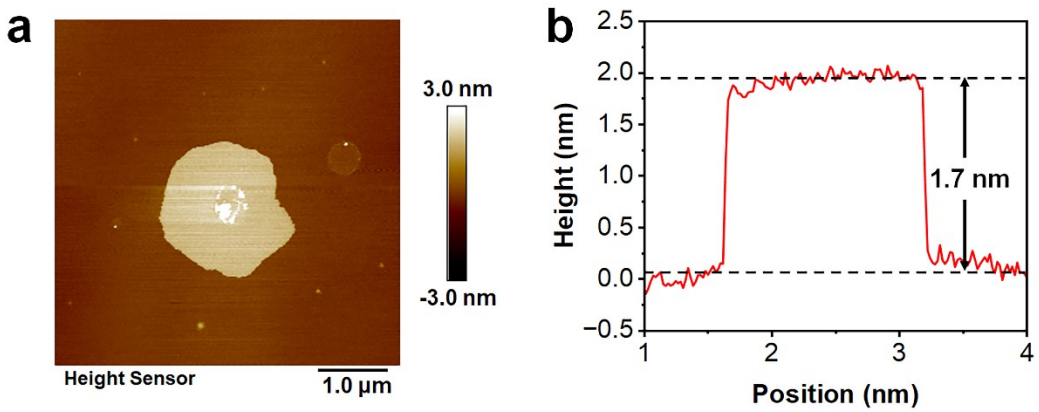

Figure S2. (a) (**a**) AFM image of Ce-BNC. (**b**) Corresponding height profile of Ce-BNC, showing a thickness of approximately 1.7 nm.

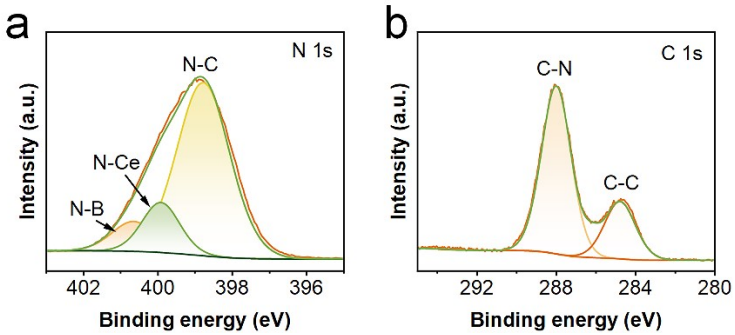

Figure S3. (a) N 1s and (b) C 1s spectra of Ce-BNC.

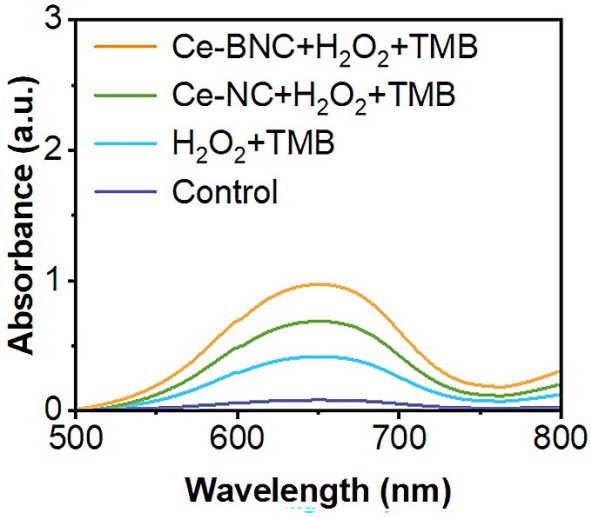

Figure S4. POD-like activity of Ce-BNC and Ce-NC.

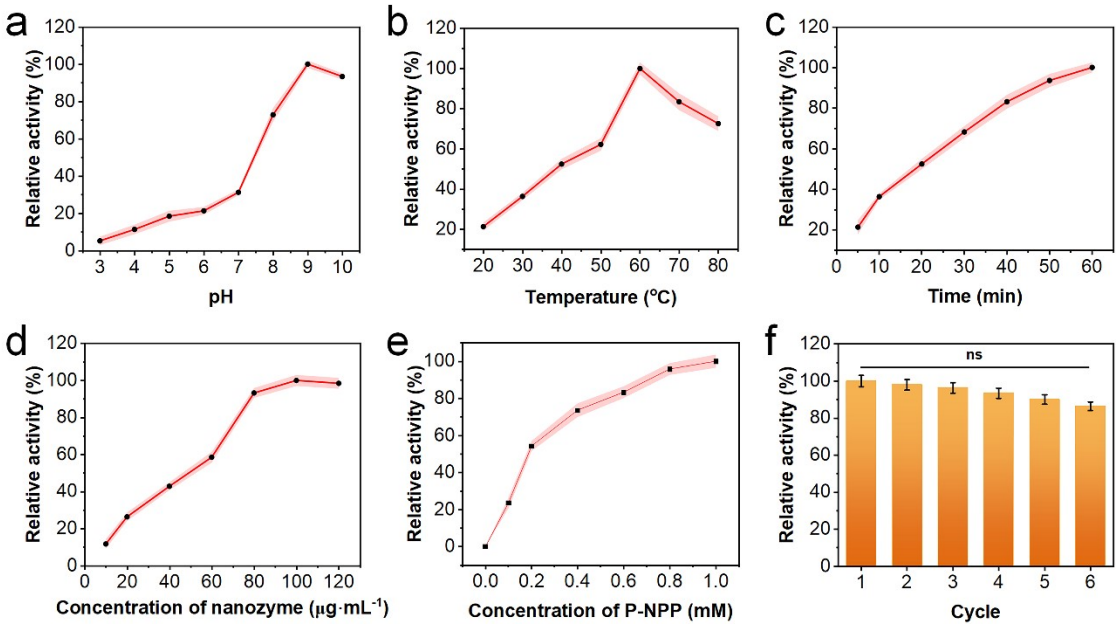

Figure S5. Effect of (a) pH, (b) temperature, (c) time, (d) concentration of nanozyme, (e) concentration of nanozyme and (f) number of cycles on OPH-like activity.

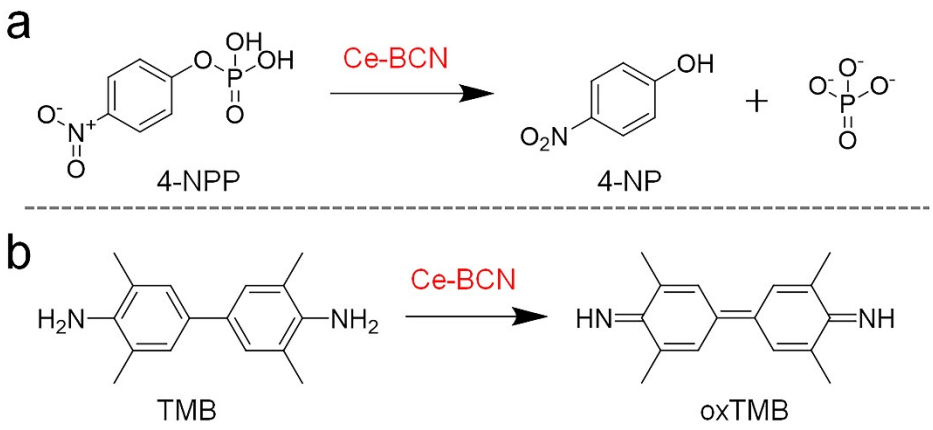

Figure S6. The chemical reaction equations of (a) 4-NPP and (b) TMB.

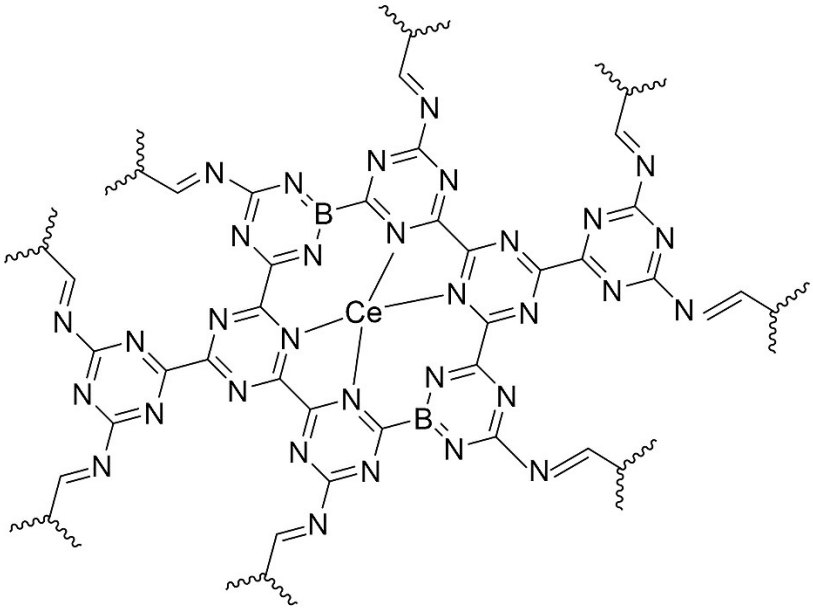

Figure S7. Schematic illustration of the Ce-BNC single-atom nanozyme.

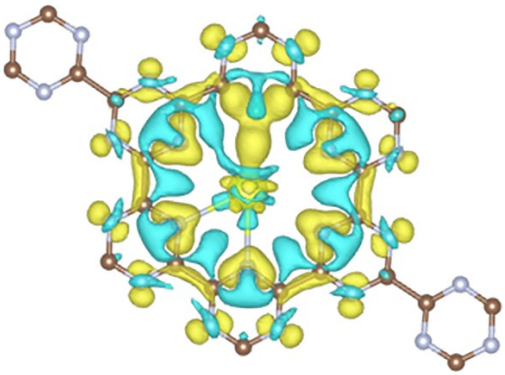

Figure S8. EDD of Ce-BNC.

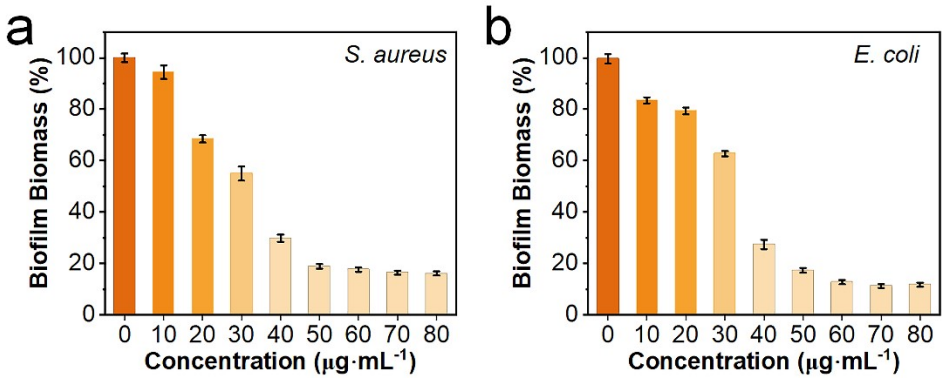

Figure S9. Concentration-dependent antibiofilm activity of Ce-BNC against biofilm-forming bacteria: (a) *S. aureus* and (b) *E. coli*.

Table S1. The catalytic parameters of different catalysts on PNPP.

Catalysts	K_m (mm)	V_{max} (m s^{-1})	K_{cat} (s^{-1})	Ref.
DCNG	0.029	7.170×10^{-7}	73.213	[1]
Ce-MOF	0.252	9.860×10^{-7}	2.310	[2]
$MOF_{-2.5Au-Ce}$	0.876	2.060×10^{-7}	343.333	[3]
ZIF-90	1.950	4.000×10^{-9}	7×10^{-4}	[4]
P2-Zn(II)	0.930	4.000×10^{-8}	7×10^{-4}	[5]
Hf-Ni	0.230	2.783×10^{-8}	1×10^{-4}	[6]
SA Ce-N-C	0.276	5.855×10^{-6}	-	[7]
Ce-NC	0.294	2.803×10^{-8}	0.028	This work
Ce-BNC	0.183	9.235×10^{-8}	1×10^{-4}	This work

References

1 Y. Xiong, L. Su, Y. Peng, S. Zhao and F. Ye, *J. Colloid Interface Sci*., 2022, **627**, 405-414.

2 X. Yuan, J. Xiong, X. Wu, N. Ta, S. Liu, Z. Li and W.-Y. Lou, *Chem. Eng. J*., 2024, **480**, 148246.

3 Z. Liu, F. Wang, J. Ren and X. Qu, *Biomaterials*., 2019, **208**, 21-31.

4 T. Fu, C. Xu, R. Guo, C. Lin, Y. Huang, Y. Tang, H. Wang, Q. Zhou and Y. Lin, *ACS Appl. Nano Mater.,* 2021, **4**, 3345-3350.

5 J. Yang, Z. Wang, W. Xiao, Y. Peng, M. Qiu, X. Xiong, Y. Lu, T. Chen and Z. Xu, *Colloids Surf. A*., 2023, **675**, 132034.

6 J. Dong, H.-D An, Z.-K Yue, S.-L. Hou, Y. Chen, Z.-J. Zhang, P. Cheng, Q. Peng and B. Zhao, *ACS Cent. Sci.*, 2021, **7**, 831-840.

7 G. Song, J.-C. Li, Z. Majid, W. Xu, X. He, Z. Yao, Y. Luo, K. Huang and N. Cheng, *Food Chem.*, 2022, **390**, 133127.